Fuel 402 (2025) 135979

Contents lists available at ScienceDirect

Fuel

journal homepage: www.elsevier.com/locate/fuel

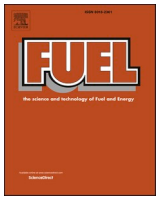

Full Length Article

Effects of cryogenic temperature on propagation of hydrogen-air rotating detonation waves

Zhaoxin Ren [a,b,*], Jie Lu [c], Wulf G. Dettmer [a,b]

[a] Department of Aerospace Engineering, Faculty of Science and Engineering, Swansea University, Swansea SA1 8EN, UK
[b] Zienkiewicz Institute for Modelling, Data and AI, Swansea University, Swansea SA1 8EN, UK
[c] School of Power and Energy, Northwestern Polytechnical University, Xi'an, China

ARTICLE INFO

Keywords:
Rotating detonation wave
Cryogenic hydrogen
Propagation
Numerical simulation

ABSTRACT

This study presents a comprehensive numerical investigation into the formation and propagation of rotating detonation waves (RDWs) in hydrogen-air mixtures at cryogenic temperatures, with the objective of evaluating the performance benefits and feasibility of using cryogenic hydrogen in propulsion systems. This represents the first reported study of RDWs fuelled by cryogenic hydrogen, a fuel of interest due to its high density and potential for high-efficiency, carbon-free combustion. The cryogenic flow is modelled using the Noble-Abel Stiffened Gas (NASG) equation of state, coupled with a detailed chemical reaction mechanism. Simulations are performed across a range of inflow total temperatures (100 K to 1000 K) and pressures (3 to 7 bar) to examine their influence on RDW dynamics. Under cryogenic conditions (100 K), the detonation pressure significantly exceeds typical Chapman-Jouguet (C-J) values. Decreasing the inflow temperature increases mixture density and turbulence intensity, leading to enhanced detonation strength and faster wave propagation. In contrast, increasing the inflow pressure moderately raises detonation pressure but has only a slight effect on wave speed. These findings demonstrate that cryogenic hydrogen enables improved detonation performance and offers a promising pathway for developing high-efficiency, low-emission rotating detonation engines (RDEs). This work lays the foundation for future experimental studies and the advancement of cryogenic detonation-based propulsion technologies.

1. Introduction

Propulsion based on detonation waves, which convert chemical energy into thermal energy, has been investigated for the past 30 years [1,2]. Due to a more efficient quasi constant-volume thermodynamic cycle, a higher specific impulse is expected in detonation-based propulsion. Rotating detonation for propulsion represents a promising advancement based on the self-sustaining propagation of a supersonic combustion wave within a confined annular structure [3]. The rotating detonation engine (RDE) features simple geometry, single ignition and other advantages [4]. Various aspects of the RDE, such as fuel injection patterns [5], mixing process [6], ignition and initiation of RDW [7], propagation modes [8], and thrust/impulse performance [9], have been studied both experimentally and numerically. However, modelling the transient flow dynamics and combustion process is complicated, particularly under cryogenic temperature and multiphase flow conditions.

Hydrogen, as a zero-carbon fuel, plays a crucial role in achieving global net-zero emissions, offering significant environmental and economic advantages. Its high density in cryogenic gas and liquid forms makes transport and storage economically favourable, and the cooling of the combustion chamber is facilitated by its extremely low temperature. The use of cryogenic hydrogen for RDEs is particularly innovative and promising. Hydrogen-fuelled detonative propulsion devices benefit from carbon-zero combustion and detonation with pressure gain. The low nitrogen oxide (NOx) emissions from detonation [10] are also advantageous. Hydrogen's long history in RDW research stems from its ease of ignition and initiation of propagating detonation waves. As a starting point for using hydrogen for rotating detonation, Hayashi et al. [11] numerically found a continuous spin detonation wave in a millimetre-level circular tube using a hydrogen/air mixture. Bykovskii et al. [12] theoretically studied the spin detonation in a two-dimension combustor. Davidenko et al. [13] used numerical simulations to investigate the processes of RDW fed with a hydrogen–oxygen mixture. From 2011, the research on rotating detonation using hydrogen started increase rapidly

* Corresponding author.
E-mail address: zhaoxin.ren@swansea.ac.uk (Z. Ren).

https://doi.org/10.1016/j.fuel.2025.135979
Received 1 May 2025; Received in revised form 2 June 2025; Accepted 11 June 2025
Available online 17 June 2025

Nomenclature

c_p	specific heat of mixture gas (J kg^{-1} K^{-1})
D_k	diffusion coefficient of k^{th} species (m^2 s^{-1})
e_t	specific total energy (J kg^{-1})
h	specific enthalpy (J kg^{-1})
m	mass (kg)
P	static pressure (Pa)
P_0	total pressure (Pa)
q	heat flux (J m^{-2} s^{-1})
R	universal gas constant (J K^{-1} mol^{-1})
S_i	source term
T	static temperature (K)
T_0	total temperature (K)
u	velocity (m s^{-1})
W	molecular weight of mixture gas (kg/mol)
Y_k	mass fraction of kth species (−)
λ	thermal conductivity (W m^{-1} K^{-1})
μ	dynamic viscosity (Pa s)
ρ	density (kg m^{-3})

[14–21]. Researchers applied experiments [22–24] and numerical simulations [25–27] on the initiation approaches, fuel injection, propagation modes, nozzle types, and specific impulse of RDW with hydrogen fuel. However, none of them touches on the hydrogen with cryogenic temperatures used for rotating detonation. In addition, the investigations by Debnath and Pandey [28–35] collectively advance the understanding of detonation combustion dynamics, particularly in hydrogen-air mixtures within pulse detonation combustors (PDCs). Their work examines key parameters such as blockage ratios, ejector configurations, fuel phase (liquid versus gaseous), and combustion/exergy efficiencies. These studies provide a robust foundation for detonation-based propulsion research. Building upon their findings, the present study extends the exploration into rotating detonation waves (RDWs) under cryogenic conditions, thereby contributing to the advancement of efficient, high-performance, and compact propulsion systems suitable for future aerospace applications.

As detonation relies on rapid exothermic reactions, a general decrease in mixture temperature leads to reduced chemical reactivity, which can significantly hinder the initiation and stability of RDW. While most RDW research focuses on highly reactive mixtures under ambient or elevated temperatures, there is interest in understanding RDWs in low-reactivity conditions, which may share key characteristics with the cryogenic hydrogen-air mixtures investigated in this study. For example, methane-air mixtures have been widely studied as low-reactivity fuels in RDEs. It has been shown that achieving stable RDW in methane-air mixtures is challenging, and initiation often fails under standard configurations. Studies have found that increasing the nozzle contraction ratio enhances the local pressure and temperature, improving the likelihood of successful detonation onset [36,37]. Alternative strategies include enriching the oxidiser (e.g., using oxygen-enriched air or pure oxygen) [38] or introducing more reactive additives such as hydrogen [39] or ethylene [40]. In addition, the initiation process in non-premixed RDWs has been shown to differ significantly from premixed systems. Fan et al. [41] used schlieren visualization to capture the transient stages of ignition, identifying three distinct phases: initiation, adjustment, and stable propagation. These studies revealed that imperfect mixing in non-premixed conditions leads to lower detonation strength and thrust output compared to premixed configurations [42,43].

Here, a brief summary of all the related research on the denotation of cryogenic hydrogen is provided. In an experiment conducted by Zitoun et al. [44], the detonation in cryogenic gaseous hydrogen–oxygen mixtures with a temperature of 123 K was directly initiated, and they found that for the lowest values of the initial pressure, a decrease in initial temperature may favour the onset of detonation. Coy et al. [45] used mixtures of hydrogen and oxygen at temperatures between 90 and 110 K and pressures from 3 to 5 bar. They found that the pressure and speed of the detonation wave become much higher than the Chapman-Jouget (C-J) pressure and speed. Jouot et al. [46] found that the propagation wave speed increases for gaseous hydrogen at 100 K, and the results are close to the results obtained by Coy et al. [45]. Regarding the deflagration wave transitioning to a detonation wave (DDT) of hydrogen at cryogenic temperatures, Kuznetsov et al. [47] conducted experiments to investigate the flame acceleration and detonation transition of hydrogen-air mixtures at cryogenic temperatures from 90 to 130 K. They concluded that the maximum combustion pressure was several times higher, and the distance to form the detonation wave was two times shorter compared to the ambient temperature conditions. Shen et al [48,49] found unstable detonation at cryogenic temperature (77 K) for hydrogen–oxygen mixtures, and for the fuel-rich mixture with low pressures from 0.2 to 0.5 atm, strong flame acceleration was observed, and the increasing initial pressure contributed to the formation of detonation.

While numerous studies have explored rotating detonation waves (RDWs) in hydrogen-air mixtures under ambient and elevated temperatures, there is currently no research addressing RDW propagation under cryogenic conditions. Existing investigations of cryogenic hydrogen detonation are limited to one-dimensional or non-rotating configurations, often focused on initiation thresholds or detonation limits. Furthermore, prior studies do not consider the effects of cryogenic temperatures on RDW structure and performance. This leaves a significant gap in understanding how cryogenic hydrogen behaves in a rotating detonation environment, which is critical for future propulsion applications using gaseous or liquid cryogenic fuels.

To fully capture the physics of cryogenic reactive flow, the calculation of thermophysical properties should consider the low-temperature regions. The Noble-Abel Stiffened (NASG) gas equation of state (EOS) [50,51] with the National Institute of Standards and Technology (NIST) database [52] will be implemented for modelling the thermophysical properties at cryogenic temperatures. A detailed chemical mechanism of hydrogen [53], considering a wide range of pressures and temperatures, is used to predict accurate ignition delays and heat release rates. A series of numerical experiments will be conducted by changing the stagnation temperatures and stagnation pressures at the inlet boundary. The pressure of the detonation wave will be analysed. The rest of the paper is organized as follows: in Section 2 and Section 3, numerical methods and physical models are presented. The numerical results are presented and discussed in Section 4. Finally, the main conclusions drawn from the work are summarized in Section 5.

This study is the first to numerically investigate the formation and self-sustained propagation of RDWs using cryogenic hydrogen-air mixtures under realistic operating conditions. By implementing the Noble-Abel Stiffened Gas (NASG) equation of state and a detailed chemical kinetic mechanism, this work captures the effects of low temperatures (as low as 100 K) on reactive flow dynamics. The study provides quantitative insights into how cryogenic conditions influence detonation pressure and wave speed, filling a crucial knowledge gap and offering a new perspective for the design of high-efficiency, cryogenic hydrogen-fuelled rotating detonation engines (RDEs).

2. Physical model

The dynamics of RDWs are simulated in a two-dimensional (2D) plane in the present study. A three-dimensional (3D) model of the annular combustor, as shown by the left figure in Fig. 1, is unwrapped and a 2D computation domain is scaled by the black dashed lines, as shown by the right Fig. 2D numerical simulations differ inherently from 3D ones due to differences in energy representation (per area in 2D

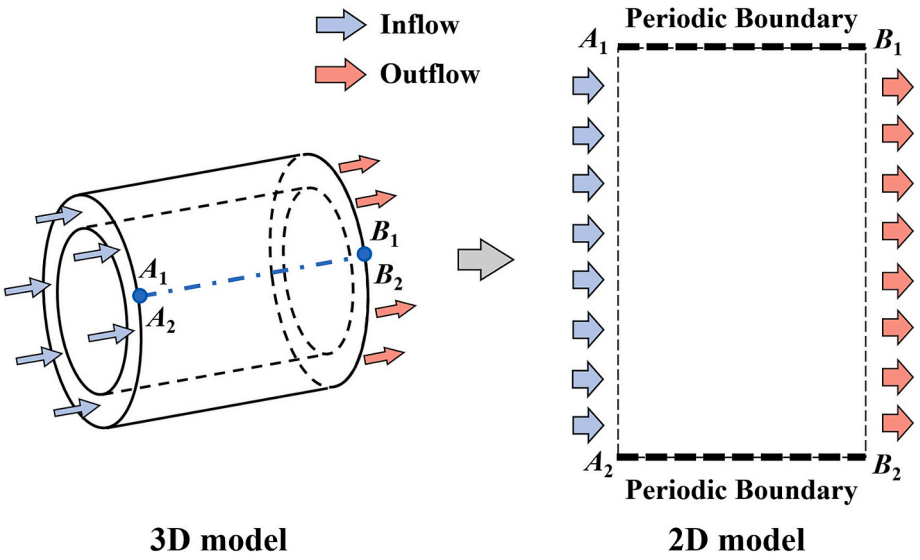

Fig. 1. Physical model and computation domain.

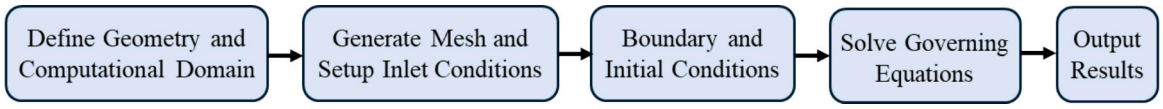

Fig. 2. Flow chart of numerical simulation.

versus per volume in 3D) and the inability of 2D models to capture certain fluid dynamics phenomena, such as boundary layer interactions and complex wave structures. As the first step in studying the dynamics of RDW in cryogenic hydrogen, we have focused on 2D simulations while neglecting the effects of wall confinement that are present in 3D cases. This approach provides foundational insights into RDW behaviour. The premixed gaseous hydrogen-air mixture is injected from the left side of the domain, which is the inlet boundary and flows out of the domain through the right boundary of the 2D chamber. The variable cross-section inlet nozzle model is applied, which is assumed to include many micro nozzles, and the inlet velocity is calculated from the local pressure [54]. The total pressure loss resulting from the nozzle expansion is considered in this model and the nozzle area ratio is 1/3. The periodic boundaries are set for the upper and lower sides of the chamber, as shown in Fig. 1. To choose a suitable computation domain and to mimic a practical application, the experiment on the operation of a rotating detonation combustor using hydrogen as the fuel [55] is referred to in this paper. The diameter of the annular chamber is 0.07 m (70 mm) and the length is 0.1 m (100 mm). Therefore, the 2D computation domain has a size of 0.21 m from A_1 to A_2, and 0.1 m from A_1 to B_1 in Fig. 1.

3. Mathematical model

The present numerical simulations solve the Navier-Stokes equations together with the mass fraction equations of chemical species for the compressible, multi-component and reactive flows, described as follows,

$$\frac{\partial}{\partial t}(\rho)+\frac{\partial}{\partial x_j}(\rho u_j)=0 \tag{1}$$

$$\frac{\partial}{\partial t}(\rho u_i)+\frac{\partial}{\partial x_j}(\rho u_i u_j+P\delta_{ij}-\tau_{ij})=0 \tag{2}$$

$$\frac{\partial}{\partial t}(\rho e_t)+\frac{\partial}{\partial x_j}\left((\rho e_t+P)u_j-u_i\tau_{ij}-q_j\right)=0 \tag{3}$$

$$\frac{\partial}{\partial t}(\rho Y_k)+\frac{\partial}{\partial x_j}(\rho Y_k u_j)+\frac{\partial}{\partial x_j}\left(\rho Y_k\left(V_{k,j}+V_j^c\right)\right)=S_{\text{combustion},k} \tag{4}$$

In the above equations, the density, velocity vector, static pressure, and total energy of the reactive mixture are represented by ρ, u_i, P, and e, respectively. Y_k and $S_{\text{combustion},\ k}$ indicate the mass fraction and production or consumption due to the reaction of species k in the mixture.

The Noble-Abel Stiffened (NASG) gas equation of state (EOS) is used to close the governing equations. It can be used to model the liquid and gas in a framework. For a single component, the NASG EOS is expressed as,

$$P=\frac{\rho(\gamma-1)e}{1-b\rho}-\gamma P_\infty \tag{5}$$

with γ being the heat capacity ratio. In the NASG EOS, two empirical constants are meant to account for departure from ideal gases; they are b, the covolume, and P_∞, a reference pressure accounting for repulsive and attractive effects between molecules, respectively. When the ideal gas is used, then $b=0$ and $P_\infty=0$, and the NASG EOS becomes the ideal gas EOS.

The kinetic theory [56] is used to model the transport parameters, including the dynamics viscosity, heat conductivity coefficient, and mass diffusion coefficient. For the thermodynamic data, the specific heat capacity at constant pressure, C_p, and the specific enthalpy are modelled using a hybrid method. In particular, the thermodynamic parameters with temperatures under 300 K, which are mainly out of the scope of NASA polynomials [57], are determined from curve-fitting NIST experimental data [52]. For temperatures higher than 300 K, the thermodynamic parameters are predicted using NASA polynomials.

A detailed chemical kinetic mechanism (9 species and 19 reversible elementary reactions) of hydrogen and air (mixture of oxygen and nitrogen) [53] is used for a wide range of temperatures (298–3000 K), pressures (0.3–150 atm), and equivalence ratios (0.25–5.0). Although this mechanism does cover temperatures under 298 K, it is found the ignition delay time and reaction rate decrease drastically as temperatures fall below 300 K. The reaction under 300 K will have a minor

influence on the overall combustion performance. The validation of this mechanism for detonation at cryogenic temperatures will be shown in the following section.

For the numerical methods, the sixth-order numerical scheme of WENO-CU6 [58] is applied to obtain a sixth-order accuracy for the convection term. The diffusion term is discretized by a sixth-order compact scheme. A third-order Runge-Kutta integration is used to get the new physical information at the new time step. These approaches have been successfully used to predict the dynamics of RDWs [59]. The flow chart of numerical simulation is shown in Fig. 2.

4. Computation set-up

Starting a rotating detonation simulation is an issue since the initial field may not be good enough to lead to a stable propagating detonation wave and the initiation condition should be properly set to achieve one-way propagation of RDW. Then it can be used to study the transient wave dynamics under various inflow conditions. In this research, a direct initiation method is utilized and a detonation wave at the Chapman-Jouguet condition is set up at the start of the computation. Then the simulation runs, and the uniform mixtures of hydrogen and air are injected into the computation domain from the modelled nozzles. The initiated detonation wave propagates to consume the reactive mixtures, allowing us to investigate the self-sustained propagation dynamics at cryogenic temperatures. The premixed hydrogen and air in the inflow are at stochiometric conditions, and the total pressure (stagnation pressure), P_0, and total temperature (stagnation temperature), T_0, of inflow are varied for achieving a comparative study. Table 1 summarizes the simulation cases. The cases T# (# is a number chosen from 1 to 3) are used to investigate the influence, with the temperature of Case T1 at a cryogenic condition of 100 K. The cases P# with different total pressures from 3 bar to 5 bar are used to analyse the influence on detonation wave propagation at cryogenic temperatures.

A grid independence study was conducted to determine the optimal resolution. Three sizes of uniform grid sizes of 12.5 μm, 25.0 μm, and 50.0 μm are applied to simulate Case T1 (inflow total temperature = 100 K). Fig. 3(a) gives the temperature fields. It was found that there is a slight difference between the two comparisons. The only difference is the shape of the vortices in the shear layer, which is an unsteady phenomenon. Even for the smallest size of 12.5 μm, there are no cellular structures.

Then we look at the pressure profiles of the detonation wave, it is found that the pressure profiles match well with each other for the simulation cases using the grid sizes of 12.5 μm and 25.0 μm, as shown in Fig. 3(b). However, for the case using the grid size of 50.0 μm, there is a difference in the peak pressures. For the combined consideration of the pressure and temperature of the combustion field, we can use the grid size of 25.0 μm for the research in this manuscript.

Therefore, a uniform mesh with a grid size of 25 μm is used to discretize the computation domain and capture the flow structures and detonation wave dynamics. A total of 16 million grids are used for each case. The time step is $\Delta t = 2 \times 10^{-9}$ s to ensure stable computation. Ten detonation cycles are achieved in the simulations for each case to obtain a quasi-steady propagation behaviour that is independent of any influence from the initial condition. The simulations are carried out using the high-performance computation (HPC) facilities at Supercomputing Wales. A single case roughly requires 86,000 core hours.

Table 1
Simulation cases.

Case #	T1	T2	T3	T4	P1	P2
T_0 (K)	100	200	500	1000	100	100
P_0 (atm)	7	7	7	7	5	3

5. Results and discussion

5.1. Model verification

The first verification considers the fluid dynamics and checks the prediction ability of the current model for cryogenic hydrogen flow. Data from NASA's critical flow experiments of cryogenic hydrogen [60] is used to compare the results from the present numerical simulations, and the mass flow rates as shown in Fig. 4(a). The mass flow rates of the releasing cryogenic hydrogen (temperature of 100 K) with initial total pressures from around 10 bar to 60 bar were measured in the experiments, and it is found that the overall agreement between predicted and measured mass fluxes was reasonably good.

The second verification considers the combustion process. Although the reaction mechanism used in the present simulation has been validated for a wide range of temperatures and pressures to describe the ignition delay times and flame speeds, it needs to be further validated by predicting the cell size of the detonation wave as it propagates in hydrogen-air mixtures at cryogenic temperatures using the current thermophysical model and detailed chemical mechanism. The detonation cell size is a measurement of the combustible mixture [47] and can be used to identify the heat release rate across the detonation wave. Compared to the cell size of the detonation wave across the reactive mixture at room temperature, the size at cryogenic temperatures is larger at fuel-lean conditions [47]. Fig. 4(b) shows the detonation cell size at different concentrations. The initial pressure for the calculation of detonation cell size is 50 atm. The cell size is measured along the direction perpendicular to the propagation direction of the detonation wave, and this corresponds to the vertical direction, consistent with the size measured in the experiments [47]. It is found that the cell size predicted by the present simulation is slightly larger than the size measured in the experiment. Fig. 5 shows the detonation cell structures at a cryogenic temperature of $T = 100$ K, constructed from the recorded maximum pressure histories. The current models can provide a reasonable cell size at different fuel concentrations.

5.2. RDW propagation in cryogenic mixtures

A detonation wave with the Chapman-Jouguet (C-J) condition is used to initiate the one-way propagation of the RDW, thus eliminating flame acceleration and detonation transition processes. Fig. 6(a) displays the snapshots of the formation process of RDW for Case T1, which uses cryogenic hydrogen-air mixtures (100 K). The initial detonation wave propagates upward (along the increasing y direction), and the reactive mixtures are injected from the left side of the combustion chamber. As the detonation wave propagates upward, the hot combustion products from the detonative combustion expand around, as shown by the snapshot at the time of 10 μs. As the detonation wave contacts the injected fuel–air mixtures at cryogenic temperatures (see dark colour areas in the figures), the propagation is suppressed as the chemical reaction rate is reduced with decreasing temperature, and the detonation wave is distorted into two parts: the wave inside the mixture with cryogenic temperature (DW_{in}) and the wave outside the cryogenic area (DW_{out}), as shown by the local enlargement at time 30 μs. It is found that the DW_{out} located in the area with higher temperature propagates faster than DW_{in}. A shear layer is formed after DW_{out} and DW_{in} due to the velocity difference. From 20 μs to 40 μs, the propagation of DW_{in} is accelerated and it exceeds the DW_{out}, which propagation is slowed down due to lack of reactive mixtures. At time 80 μs, the two waves merge with each other as the reactive mixtures are continuously fed into the domain and a straight detonation wave is finally found to propagate stably upward in the chamber. Then at time 100 μs, the detonation wave encounters the initial hot combustion products, scaled by the yellow-coloured area, and continuously rotates in the domain. A typical structure of rotation detonation, which includes a quasi-normal detonation wave (RDW), an oblique shock wave (OSW), and a shear layer after the

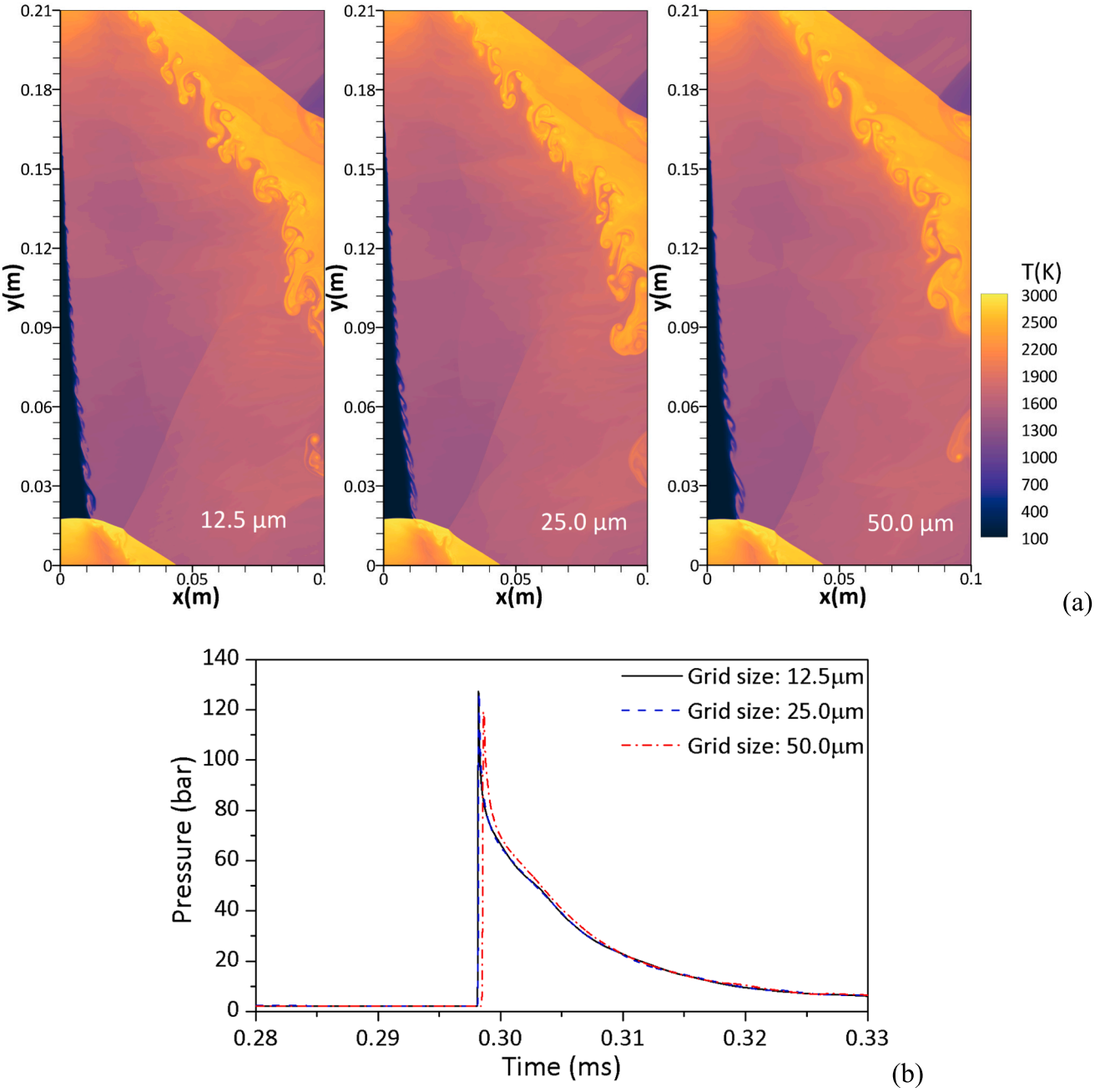

Fig. 3. Temperature fields at the same time with grid sizes (a) and pressure profiles across the detonation waves using three grid sizes (b).

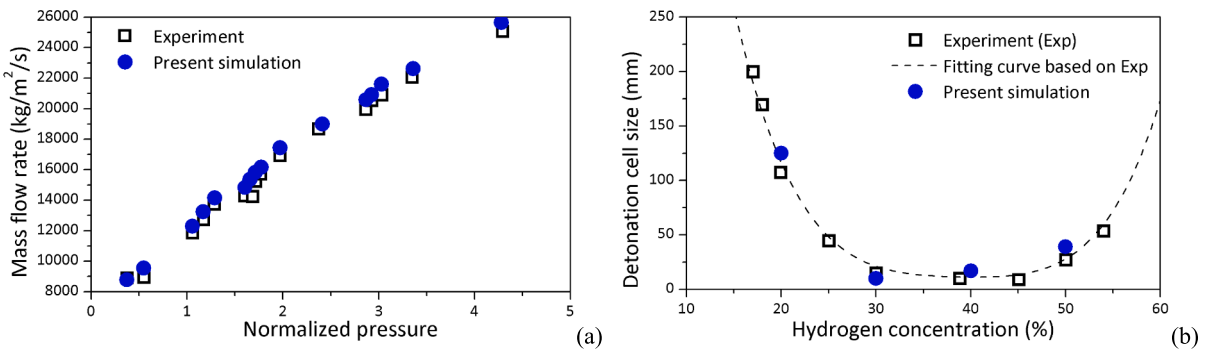

Fig. 4. Verification tests: (a) comparison of NASA's cryogenic hydrogen release experiment data [60] and present simulation results, and (b) detonation cell size of cryogenic hydrogen (T = 100 K) at different concentrations.

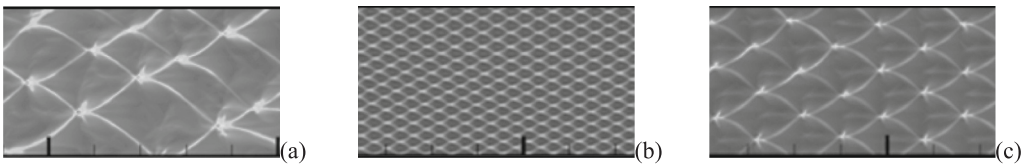

Fig. 5. Numerical detonation cell structures at cryogenic temperature (T = 100 K) for hydrogen concentrations of 20 % (a), 40 % (b), and 50 % (c).

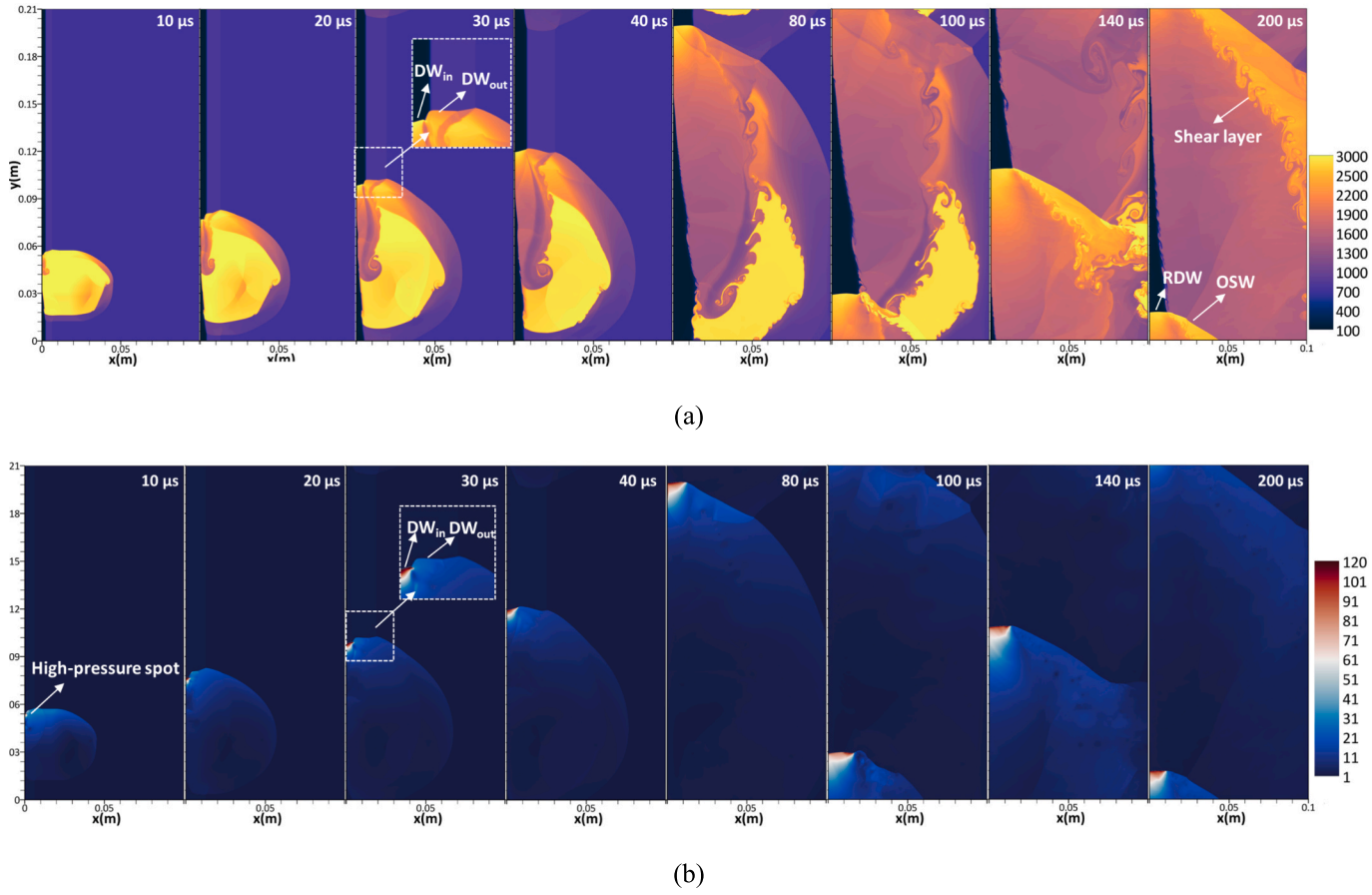

Fig. 6. Formation and propagation of rotating detonation wave for Case T1: (a) instantaneous distributions of temperature (K) and (b) instantaneous distributions of pressure (bar). Time from left to right: 10 μs, 20 μs, 30 μs, 40 μs, 80 μs, 100 μs, 140 μs, 200 μs.

two waves, is observed at 200 μs.

Fig. 6(b) displays the static pressure fields during the initiation stage of the rotating detonation for Case T1. As the initial detonation wave propagates upward, it interacts with the cryogenic reactive mixture injected from the inlet at the left boundary, forming a local high-pressure spot at time 10 μs (see Fig. 6). Then the high-pressure area expands towards the right direction as the fuel–air mixture flows from the inlet to the right. The distorted pressure wave clearly has two parts, a reacting wave across the cryogenic mixture, DW_{in}, and a non-reacting wave outside the fuel-filling region, DW_{out}. The reactive wave with

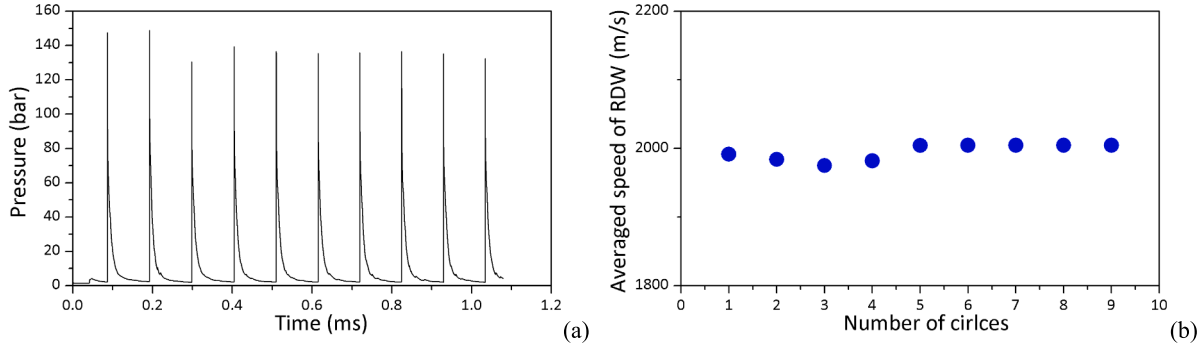

Fig. 7. Pressure variation at a fixed observation point (a) and associated averaged detonation speed (b) for Case T1.

high pressure expands towards the right side as it propagates upward, finally forming a stable detonation wave that rotates continuously in the combustion chamber.

After tracking the pressure signals at a fixed observation point near the inlet of the combustion chamber, it is proven that a stable detonation wave can be generated and then rotated continuously in the cryogenic hydrogen-air mixtures, as shown in Fig. 7(a). After an initial oscillation process of pressure, the peak value stabilizes around 130 to 140 bars. Using the time between two neighbouring pressure peaks and the length of the combustor, the local averaged speed of the detonation wave is calculated. Similar to the pressure profiles, the propagation speed of the RDW becomes quasi-constant after around four circles of wave rotation in the combustor. Given that the C-J detonation pressure of stoichiometric hydrogen-air mixture is approximately 16 to 20 bar [61], the pressure of the RDW formed at cryogenic temperature is found to be much higher, confirming the phenomenon observed in the experimental study on detonation transition at cryogenic temperatures [47]. Considering the propagation speed of the RDW, the C-J detonation speed is approximately 1960 to 2000 m/s [61], and the present results indicate that the RDW at cryogenic temperatures, as shown in Fig. 7(b), maintains a similar propagation speed. Therefore, based on the numerical tests, we can conclude that cryogenic temperature can have a significant impact on the detonation pressure. This is mainly due to the increasing Reynolds numbers (increasing turbulence intensity) with increasing flow density (decreasing flow temperature) [47]. In the next section, different premixing temperatures will be chosen, and the effects on the propagation of RDW will be analysed.

5.3. Effects of inflow temperatures

To better understand the influence of premixing temperatures on RDW propagation, the inflow temperatures are increased from 100 K to 1000 K, ranging from cryogenic temperature, room temperature to high-temperature conditions. Fig. 8 shows the temperature fields of cases T1 to T4 in the combustion chamber after the RDW achieves stable propagation. Fig. 9 provides the temperature variation at an observation point near the inlet. Although the inflow reactive mixtures have different temperatures, it is found that the temperatures of the combustion products after the RDW are similar for the four cases, as shown by the peak values in Fig. 9. This indicates that the cryogenic temperatures of the inflow do not have an obvious influence on the temperatures of the detonation products. However, the overall temperature distributions in Fig. 8 show that Case T4 with hot inflows has the highest temperature fields. This is mainly due to the fact that the combustion

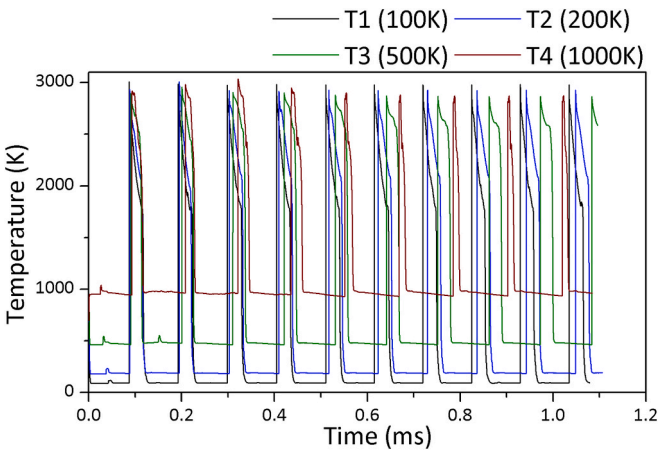

Fig. 9. Temperature variation at a fixed observation point for Cases T1 (black), T2 (blue), T3 (green), and T4 (red). (For interpretation of the references to colour in this figure legend, the reader is referred to the web version of this article.)

products after the RDW will mix with the inflow and the decreasing inflow temperatures will reduce the average temperature in the whole computation domain. Under the influence of the cryogenic inflow for Case T1, it is observed that there is a non-uniform temperature distribution, as depicted in Fig. 8(a). It is also found that the height of the RDW with a curved shape is longer for Case T4, and decreasing premixing temperature leads to a shorter RDW.

Furthermore, Fig. 10 provides the static pressure fields from the simulations of cases T1 to T4 at the same time. It is clear that as the premixing temperature of the inflow reactants increases from Case T1 (100 K) to Case T4 (1000 K), there is a decrease in the detonation pressure and an increase in the height of the detonation wave. The pressure at the outlet of the combustion chamber is highest for Case T1, indicating that the potential contribution to the output power could be highest for using cryogenic reactants. As the snapshots are taken at the same time, the different locations of the RDW indicate that the propagation speed of the detonation waves in reactive mixtures with different temperatures varies.

The pressure signals in Fig. 11 reflect that the RDW for Case T1 propagates faster than the waves for other cases inside the combustion chamber. Increasing the inlet premixing temperature not only leads to a slower detonation speed but also results in a lower detonation pressure.

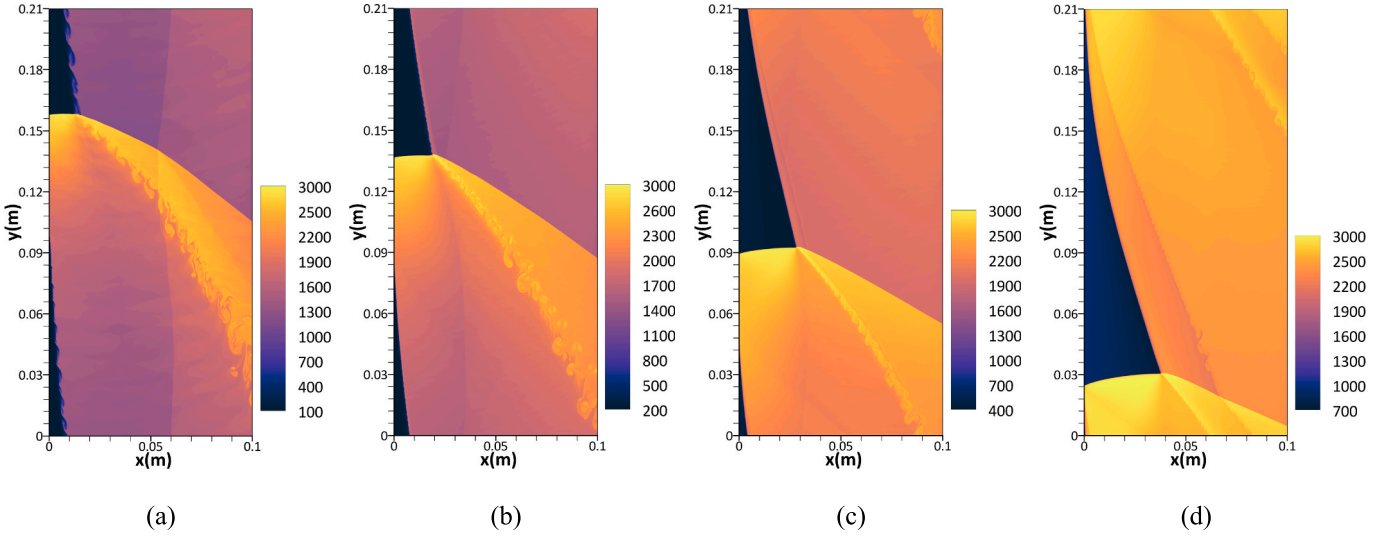

Fig. 8. Instantaneous distributions of temperature (K) at the same time: (a) Case T1, (b) Case T2, (c) Case T3, and (d) Case T4.

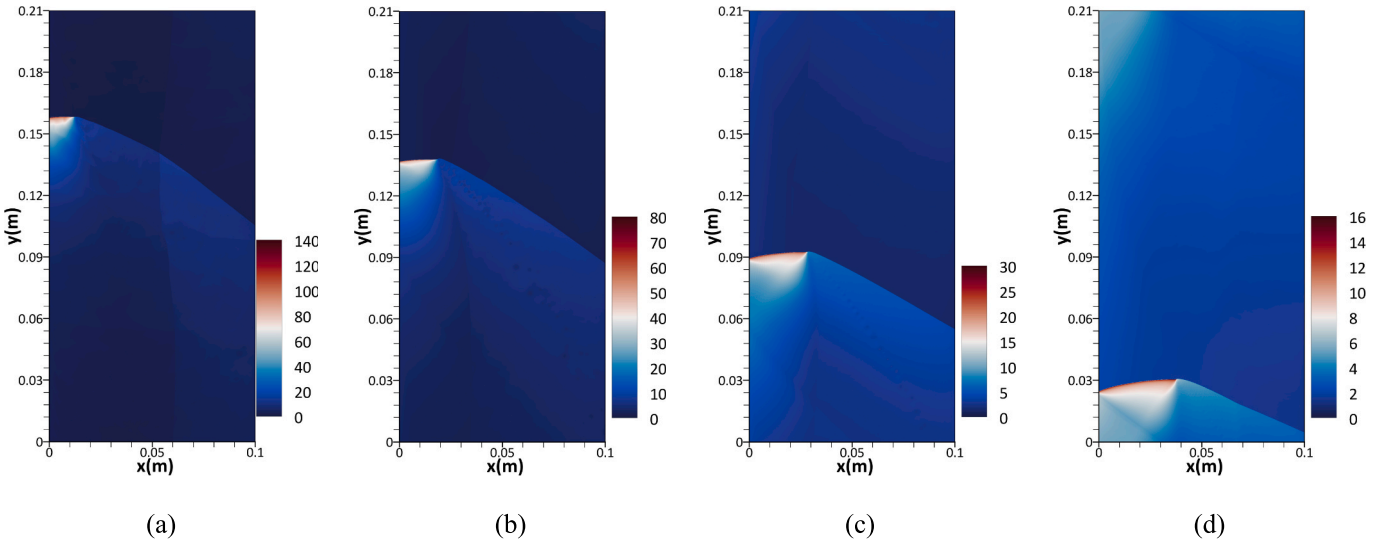

Fig. 10. Instantaneous distributions of pressure (bar) at the same time: (a) Case T1, (b) Case T2, (c) Case T3, and (d) Case T4.

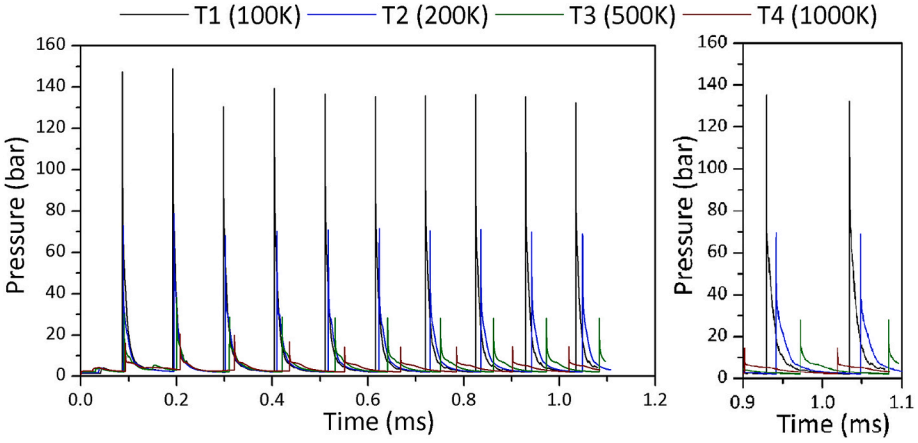

Fig. 11. Pressure variation at a fixed observation point for Cases T1 (black), T2 (blue), T3 (green), and T4 (red). The right figure is an enlargement of one rotation circle between two neighbouring pressure peaks. (For interpretation of the references to colour in this figure legend, the reader is referred to the web version of this article.)

From the enlargement of the pressure profiles during one rotating circle, it is found that the pressure of the RDW for Case T1 is almost two times higher than the pressure of the RDW for Case T2 with a higher inflow temperature of 200 K. This feature was confirmed in the experimental investigation on the deflagration to detonation transition of cryogenic hydrogen [47], mainly attributed to the increasing density and the associated increasing Reynolds number in the mixtures with lower temperatures. As the premixing temperature further increases to 500 K for Case T3, the denotation pressure drops significantly to half of the pressure peaks for Case T2, and there is an even decrease from Case T3 to Case T4 with 100 K. Here we can conclude that low-temperature premixing conditions before the reactants enter the combustion chamber may contribute to a higher detonation pressure and a faster detonation wave, which means a higher frequency and is beneficial to have the potentiality to improve the thermodynamic efficiency [1] and hence engine performance.

Fig. 12 shows the post-processed averaged speed of the RDW in different cases to investigate the effects of inflow temperatures. There is a slight difference in the speed of the detonation wave between Case T1 and Case T2. As the inflow temperature increases to 500 K, it is observed that the speed decreases obviously to around 1900 m/s. The propagation of the RDW becomes even slower as the inflow temperature increases to

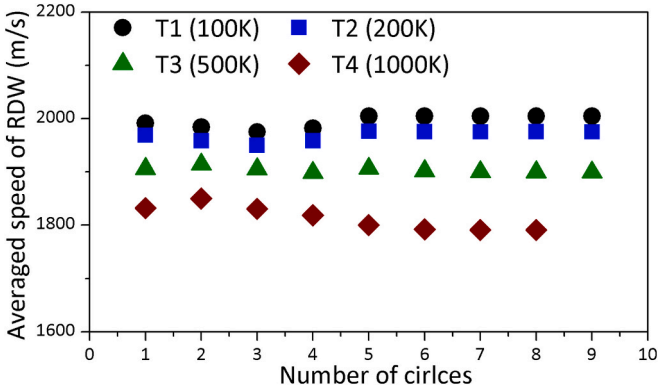

Fig. 12. Averaged speed of detonation waves at different rotating circles for Cases T1, T2, T3, and T4.

1000 K for Case T4. In the experimental study on the detonation transition of cryogenic hydrogen gas [47], it was found that faster flame acceleration in the cryogenic mixture is independent of reduced chemical reactivity at low temperature, and a shorter detonation transition

distance at cryogenic temperature than that at ambient temperature. The present simulation with a wider temperature range displays similar features of the detonation wave, where decreasing temperature leads to increasing propagation speed of detonation waves.

Increasing inlet total temperatures from 100 K, 200 K, 500 K to 1000 K contributes to higher combustion product temperatures and more uniform temperature distributions in the combustion chamber. In contrast, lower inflow temperatures lead to increasing detonation pressures and faster propagation speeds, which can potentially improve the thermodynamic efficiency of the engine when cryogenic hydrogen is used.

5.4. Effects of inflow pressures

The inflow total pressures, P_0, are decreased from 7 bar (Case T) to 5 bar (Case P1) and further 3 bar (Case P2) to analyse the pressure's influence on the RDW propagation in cryogenic flows. It should be mentioned that the inflow mass flow rate increases as P_0 increases. The inflow total temperatures, T_0, are kept the same as 100 K in the three cases. From the distributions of the temperatures in the combustion chamber (Fig. 13), it is found that the change in inflow pressure has slight influences on the combustion fields. The difference in the flow structures exists in the shear layers after the detonation wave and the oblique shock wave, and the lower pressures result in larger vortices in the shear layers.

The pressure contours indicate the wave structures of rotating detonation maintain a similar pattern as the inflow pressure decreases from Case T1 to Case P2, as shown in Fig. 14. From the location of the detonation wave, the propagation speeds of the RDW are very similar. Therefore, the inflow pressures have negligible influence on the wave dynamics. The only difference is the detonation pressure, and the decrease in inflow pressure results in the reduced pressure of the RDW.

Fig. 14 displays the pressure signals for Cases T1, P2 and P3 to analyse the propagation speed and pressure of the RDW. From the locations of the pressure peaks, it is very hard to identify the difference in the propagation speed. It is found the detonation waves have the same speed in the first few rotating circles at the locations of the pressure peaks are the same. As the RDW continues propagating in the combustion chamber, it can be observed that Case T1, with a higher inflow pressure, has a slight acceleration, and the pressure peaks appear a little earlier, as shown in the right part of Fig. 14, but this difference can be neglected. The increase in inflow pressures contributes to the slight acceleration of RDW propagation. The major influence of the inflow pressure is detonation pressure, namely the increasing inflow pressure

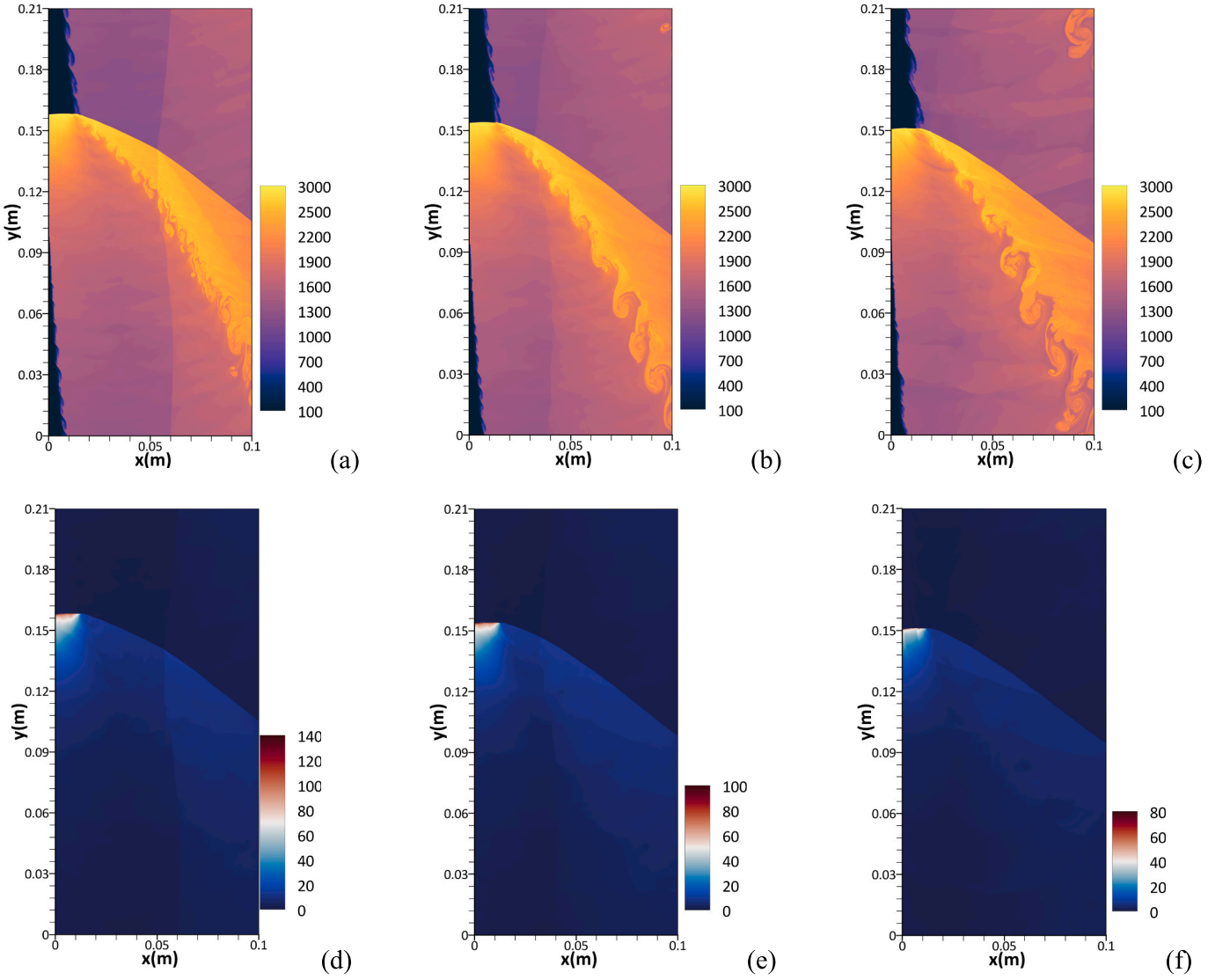

Fig. 13. Instantaneous distributions of temperature (K) at the same time: (a) Case T1, (b) Case P1, and (c) Case P2, and Instantaneous distributions of pressure (bar) at the same time: (d) Case T1, (e) Case P1, and (f) Case P2.

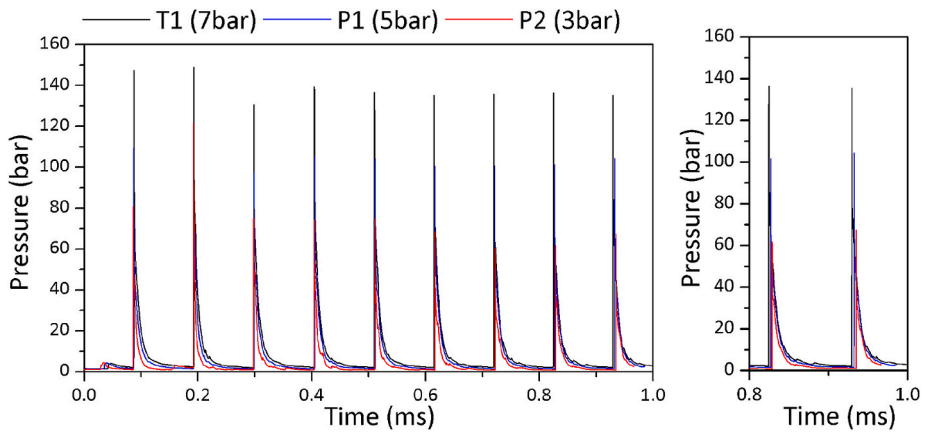

Fig. 14. Pressure variation at a fixed observation point for Cases T1 (black), P1 (blue), and P2 (red). (For interpretation of the references to colour in this figure legend, the reader is referred to the web version of this article.)

leads to an increase in detonation pressure.

Decreasing inflow total pressures from 7 bar to 3 bar shows negligible influence on wave dynamics but results in reduced detonation pressure. The speed of the detonation wave remains similar across different pressures, with higher inflow pressure contributing to slight acceleration.

5.5. Practical applications

The findings of this study have direct relevance to the development of next-generation aerospace propulsion systems. The demonstrated performance advantages of cryogenic hydrogen-fuelled rotating detonation can be exploited in reusable launch vehicles, upper-stage rocket engines, and high-speed air-breathing propulsion systems such as scramjets. The significantly elevated detonation pressures and propagation speeds observed under cryogenic conditions indicate the potential for more compact, lightweight, and thermodynamically efficient propulsion architectures.

Furthermore, the use of hydrogen in its cryogenic state not only enhances combustion performance but also facilitates high-density fuel storage, which is particularly advantageous for volume-constrained aerospace and space systems. These attributes also support the development of advanced energy conversion systems in spacecraft, defence technologies, and next-generation power units where high thrust-to-weight ratios and compactness are essential.

6. Conclusions

This study presents the first comprehensive numerical investigation into the formation and propagation of rotating detonation waves (RDWs) in cryogenic hydrogen-air mixtures. A hybrid numerical framework was developed, combining the compressible Navier-Stokes equations, the Noble-Abel Stiffened Gas (NASG) equation of state, and a detailed chemical kinetic mechanism. Simulations were performed across inflow temperatures ranging from 100 K to 1000 K and pressures from 3 to 7 bar. The key findings and mechanistic insights are summarised as follows:

(1) Enhanced detonation strength at cryogenic conditions:
At 100 K and 7 bar, the detonation pressure reached 130–140 bar, far exceeding the Chapman-Jouguet (C-J) pressure. This enhancement is attributed not only to the initial thermodynamic state but also to intensified energy release and compression effects driven by the high-density inflow.
(2) Fine-scale dynamics captured by high grid resolution:
A grid resolution of 25 μm was used to resolve sharp gradients and small-scale structures such as shear layers, vortex roll-up, and localised hotspots. These features are essential for capturing auto-ignition, shock-flame interaction, and instability mechanisms, which are particularly under cryogenic conditions, where chemical reactivity is reduced but turbulence is intensified due to higher flow density.
(3) Cryogenic temperatures influence detonation mechanism:
Lower inflow temperatures result in higher density and Reynolds number, which enhance turbulence and fuel-oxidiser mixing near the reaction front. This turbulence-induced transport offsets the slower chemical kinetics at low temperatures, enabling stable wave propagation and higher pressure gain.
(4) Limited role of inflow pressure in wave speed:
While increasing the total inflow pressure moderately raises the detonation pressure, its impact on wave speed is negligible. This indicates that RDW propagation is primarily governed by the thermochemical state of the mixture rather than its inertial properties.

These results highlight the potential of cryogenic hydrogen as a high-performance, zero-carbon fuel for rotating detonation engines (RDEs). The observed thermodynamic and fluid dynamic advantages offer promising avenues for the development of compact, efficient, and sustainable propulsion systems. Potential applications include space launch systems, reusable upper-stage propulsion, and hypersonic air-breathing vehicles. The findings also underscore the importance of high-fidelity simulations in capturing the underlying physical mechanisms of detonation stability and performance under extreme conditions.

CRediT authorship contribution statement

Zhaoxin Ren: Writing – review & editing, Writing – original draft, Validation, Project administration, Methodology, Investigation, Funding acquisition, Formal analysis, Conceptualization. **Jie Lu:** Writing – review & editing, Visualization, Validation, Methodology, Formal analysis. **Wulf G. Dettmer:** Writing – review & editing, Formal analysis.

Declaration of competing interest

The authors declare that they have no known competing financial interests or personal relationships that could have appeared to influence the work reported in this paper.

Acknowledgements

The authors thank Supercomputing Wales for its high-performance

computation facilities. This research is partially funded by EPSRC PBIAA: The Switch to Net Zero Buildings.

Data availability

Data will be made available on request.

References

[1] Wolański P. Detonative propulsion[J]. Proc Combust Inst 2013;34(1):125–58.
[2] Zhang H, Ng HD, Chen Z, et al. Hydrogen flame and detonation physics[J]. Phys Fluids 2024;36(3).
[3] Raman V, Prakash S, Gamba M. Nonidealities in rotating detonation engines[J]. Annu Rev Fluid Mech 2023;55:639–74.
[4] Qiu Y, Wu Y, Huang Y, et al. Heat transfer characteristics of H2/air rotating detonation combustor[J]. Phys Fluids 2024;36(1).
[5] Sheng Z, Cheng M, Wang JP. Multi-wave effects on stability and performance in rotating detonation combustors[J]. Phys Fluids 2023;35(7).
[6] Yang X, Song F, Wu Y, et al. Experimental investigation on the performance of the variable cross section rotating detonation engine[J]. Phys Fluids 2023;35(8).
[7] Han C, Bian J, Shi B, et al. Numerical investigation of detonation initiation in a modeled rotating detonation engine[J]. Phys Fluids 2024;36(1).
[8] Zhao T, Zhu J, Ling M, et al. Coupling characteristic analysis and propagation direction control in hydrogen–air rotating detonation combustor with turbine[J]. Int J Hydrogen Energy 2023;48(58):22250–63.
[9] Yokoo R, Goto K, Kim J, et al. Propulsion performance of cylindrical rotating detonation engine[J]. AIAA J. 2020;58(12):5107–16.
[10] Van Beck C, Raman V. NOx formation processes in rotating detonation engines[J]. Front Aerosp Eng 2024;3:1335906.
[11] Tsuboi N, Eto K, Hayashi AK. Three-dimensional numerical simulation of H2/air detonation in a circular tube: structure of spinning mode[C]. In: 20th International Colloquium on the Dynamics of Explosions and Reactive Systems; 2005. p. 71.
[12] Zhdan SA, Bykovskii FA, Vedernikov EF. Mathematical modeling of a rotating detonation wave in a hydrogen-oxygen mixture[J]. Combust Explos Shock Waves 2007;43:449–59.
[13] Davidenko DM, Gökalp I, Kudryavtsev AN. Numerical modeling of the rotating detonation in an annular combustion chamber fed with hydrogen-oxygen mixture [C]. Proceedings of the European Combustion Meeting. 2007.
[14] Yi TH, Lou J, Turangan C, et al. Propulsive performance of a continuously rotating detonation engine[J]. J. Propul. Power 2011;27(1):171–81.
[15] Schwer D, Kailasanath K. Numerical investigation of the physics of rotating-detonation-engines[J]. Proc Combust Inst 2011;33(2):2195–202.
[16] Kindracki J, Kobiera A, Wolański P, et al. Experimental and numerical study of the rotating detonation engine in hydrogen-air mixtures[J]. Prog Propul Phy 2011;2:555–82.
[17] Kindracki J, Wolański P, Gut Z. Experimental research on the rotating detonation in gaseous fuels–oxygen mixtures[J]. Shock Waves 2011;21:75–84.
[18] Kailasanath K. The rotating detonation-wave engine concept: a brief status report [C]. In: 49th AIAA aerospace sciences meeting including the new horizons forum and aerospace exposition; 2011. p. 580.
[19] Yamada T, Hayashi AK, Yamada E, et al. Detonation limit thresholds in H2/O2 rotating detonation engine[J]. Combust Sci Technol 2010;182(11–12):1901–14.
[20] Pan Z, Fan B, Zhang X, et al. Wavelet pattern and self-sustained mechanism of gaseous detonation rotating in a coaxial cylinder[J]. Combust Flame 2011;158(11):2220–8.
[21] Yamada T, Uemura Y, Tsuboi N, et al. Physics of detonation propagation in rotating detonation Engine[J]. Proceedings of the 23rd ICDERS. 2011.
[22] Liu SJ, Lin ZY, Liu WD, et al. Experimental realization of H2/air continuous rotating detonation in a cylindrical combustor[J]. Combust Sci Technol 2012;184(9):1302–17.
[23] Fotia ML, Schauer F, Kaemming T, et al. Experimental study of the performance of a rotating detonation engine with nozzle[J]. J Propul Power 2016;32(3):674–81.
[24] Han J, Bai Q, Zhang S, et al. Experimental study of H2/air rotating detonation wave propagation characteristics at low injection pressure[J]. Aerosp Sci Technol 2022;126:107628.
[25] Gaillard T, Davidenko D, Dupoirieux F. Numerical simulation of a rotating detonation with a realistic injector designed for separate supply of gaseous hydrogen and oxygen[J]. Acta Astronaut 2017;141:64–78.
[26] Jourdaine N, Tsuboi N, Ozawa K, et al. Three-dimensional numerical thrust performance analysis of hydrogen fuel mixture rotating detonation engine with aerospike nozzle[J]. Proc Combust Inst 2019;37(3):3443–51.
[27] Nassini PC, Andreini A, Bohon MD. Characterization of refill region and mixing state immediately ahead of a hydrogen-air rotating detonation using LES[J]. Combust Flame 2023;258:113050.
[28] Debnath P, Pandey KM. Numerical investigation of detonation combustion wave in pulse detonation combustor with ejector[J]. J Appl Fluid Mech 2017;10(2):725–33.
[29] Debnath P, Pandey KM. Exergetic efficiency analysis of hydrogen–air detonation in pulse detonation combustor using computational fluid dynamics[J]. Int J Spray Combust Dynamic 2017;9(1):44–54.
[30] Debnath P, Pandey KM. Numerical analysis of detonation combustion wave in pulse detonation combustor with modified ejector with gaseous and liquid fuel mixture[J]. J Therm Anal Calorim 2021;145(6):3243–54.
[31] Debnath P, Pandey KM. Numerical investigation on detonation combustion waves of hydrogen-air mixture in pulse detonation combustor with blockage[J]. Adv Aircraft Spacecraft Sci 2023;10(3):203–22.
[32] Debnath P, Pandey KM. Numerical studies on detonation wave in hydrogen-fueled pulse detonation combustor with shrouded ejector[J]. J Braz Soc Mech Sci Eng 2023;45(2):104.
[33] Debnath P, Pandey KM. Numerical analysis on detonation wave and combustion efficiency of pulse detonation combustor with U-shape combustor[J]. J Therm Sci Eng Appl 2023;15(10):101006.
[34] Debnath P, Pandey KM. Exergetic and thermal performance analysis of liquid and gaseous fuel–air mixture in PDC using computational fluid dynamics[J]. Arab J Sci Eng 2024:1–16.
[35] Debnath P, Pandey KM. Computational analysis of shrouded ejector effect on starting vortex and combustion efficiency in pulse detonation combustor with different fuels[J]. Combust Sci Technol 2025;197(5):976–98.
[36] Peng HY, Liu WD, Liu SJ, et al. Realization of methane-air continuous rotating detonation wave[J]. Acta Astronaut 2019;164:1–8.
[37] Liu SJ, Huang SY, Peng HY, et al. Characteristics of methane-air continuous rotating detonation wave in hollow chambers with different diameters[J]. Acta Astronaut 2021;183:1–10.
[38] Liu P, Wang Y, Zhang X, et al. Experimental study on upstream pressure characteristics of rotating detonation engine with methane and oxygen-enriched air[J]. Aerosp Sci Technol 2024;153:109431.
[39] Yang X, Song F, Wu Y, et al. Investigation of rotating detonation fueled by a methane–hydrogen–carbon dioxide mixture under lean fuel conditions[J]. Int. J. Hydrogen Energy 2020;45(41):21995–2007.
[40] Wang Y, Le J. A rotating detonation engine using methane-ethylene mixture and air[J]. Acta Astronaut 2021;188:25–35.
[41] Fan W, Peng H, Liu S, et al. Initiation process of non-premixed continuous rotating detonation wave through Schlieren visualization[J]. Combust Flame 2024;265:113437.
[42] Sato T, Raman V. Detonation structure in ethylene/air-based non-premixed rotating detonation engine[J]. J Propul Power 2020;36(5):752–62.
[43] Sun J, Zhou J, Liu S, et al. Numerical investigation of a rotating detonation engine under premixed/non-premixed conditions[J]. Acta Astronaut 2018;152:630–8.
[44] Zitoun R, Desbordes D, Guerraud C, et al. Direct initiation of detonation in cryogenic gaseous H2-O2 mixtures[J]. Shock Waves 1995;4(6):331–7.
[45] Coy E, Watts J, Palaniswamy S. Cryogenic, multiphase, hydrogen-oxygen detonations[C]. 43rd AIAA Aerospace Sciences Meeting and Exhibit. 2005: 1462..
[46] Jouot F, Dupre G, Quilgars A, et al. Experimental study of detonation in a cryogenic two-phase H2–O2 flow. Proc Combust Inst 2011;33(2):2235–41.
[47] Kuznetsov M, Denkevits A, Veser A, et al. Flame propagation regimes and critical conditions for flame acceleration and detonation transition for hydrogen-air mixtures at cryogenic temperatures[J]. Int J Hydrogen Energy 2022;47(71):30743–56.
[48] Shen X, Fu W, Liang W, et al. Strong flame acceleration and detonation limit of hydrogen-oxygen mixture at cryogenic temperature[J]. Proc Combust Inst 2023;39(3):2967–77.
[49] Shen X, Fu W, Zhang S, et al. Flame acceleration, detonation limit and heat loss for hydrogen-oxygen mixture at cryogenic temperature of 77 K[J]. Int J Hydrogen Energy 2024;56:1361–70.
[50] Boivin P, Cannac MA, Le Métayer O. A thermodynamic closure for the simulation of multiphase reactive flows[J]. Int J Therm Sci 2019;137:640–9.
[51] Deng X, Boivin P. Diffuse interface modelling of reactive multi-phase flows applied to a sub-critical cryogenic jet[J]. App Math Model 2020;84:405–24.
[52] Linstrom PJ, Mallard WG. The NIST chemistry WebBook: a chemical data resource on the internet[J]. J Chem Eng Data 2001;46(5):1059–63.
[53] Li J, Zhao Z, Kazakov A, et al. An updated comprehensive kinetic model of hydrogen combustion[J]. Int J Chem Kinet 2004;36(10):566–75.
[54] Fievisohn RT, Yu KH. Steady-state analysis of rotating detonation engine flowfields with the method of characteristics[J]. J Propul Power 2017:89–99.
[55] Xie Q, Wen H, Li W, et al. Analysis of operating diagram for H2/Air rotating detonation combustors under lean fuel condition[J]. Energy 2018;151:408–19.
[56] Poling BE, Prausnitz JM, O'connell JP. The properties of gases and liquids[M]. New York: Mcgraw-hill; 2001.
[57] Burcat A, Ruscic B. Third millenium ideal gas and condensed phase thermochemical database for combustion (with update from active thermochemical tables)[R. Argonne, IL (United States): Argonne National Lab. (ANL); 2005.
[58] Hu XY, Wang Q, Adams NA. An adaptive central-upwind weighted essentially non-oscillatory scheme[J]. J Comput Phys 2010;229(23):8952–65.
[59] Ren Z, Sun Y, Wang B. Propagation behaviors of the rotating detonation wave in kerosene–air two-phase mixtures with wide equivalence Ratios[J]. Flow Turbul Combust 2023;110(3):735–53.
[60] Simoneau RJ, Hendricks RC. Two-phase choked flow of cryogenic fluids in converging-diverging nozzles[R]. NASA Technical Reports 1484; 1979.
[61] Shepherd JE. Detonation in gases[J]. Proc Combust Inst 2009;32(1):83–98.